Optical investigation on pre-strike arc characteristics in medium-voltage load break switches

Naghme Dorraki, and Kaveh Niayesh

Department of Electric Power Engineering, NTNU, Trondheim, Norway

Email: naghme.dorraki@ntnu.no

Received xxxxxx
Accepted for publication xxxxxx
Published xxxxxx

Abstract

Medium Voltage Load Break Switches (MV-LBS) should pass fault current while closing and be able to re-open for the next operation. Replacing SF_6 as a high impact greenhouse insulating gas with air, makes the switch design more challenging because of the higher pre-strike arcing time and energy dissipation between contacts which leads to more contact surfaces' erosion and even higher possibility of welding. In this paper, a synthetic test circuit is used to emulate stresses applied to MV-LBS during the making of short-circuit currents. Since there are difficulties in accurate direct measurement of arc voltage because of the inherent response of the measurement system, an alternative method using Optical Emission Spectroscopy (OES) is proposed. OES measures the pre-strike arc temperature distribution profile close to the cathode surface at a test voltage of 18 kV and a making current of 17 kA. The arc electrical characterization is achieved using obtained spectroscopy results, Lowke's model, and thermal air plasma transport properties. A maximum arc temperature of 12500 K while the arc moves from the lower part of the cathode to the center, arc voltage of 30-58 V, and dissipated energy of 79-87 J are calculated for the pre-strike arc considering the impact of copper evaporated from the contact surfaces. Different arc behavior is observed in closing the contacts compared to free-burning arcs, which indicates gas flow blowing the arc caused by the contact movement. This investigation could be used for a better understanding of switching behavior and efficient control of the operation.

Keywords: load break switch, medium voltage, arc erosion, electrical contacts, arc-material interaction, optical emission spectroscopy, arc diagnostics

1. Introduction

Arc burning in Medium Voltage Load Break Switches (MV-LBS) directly affects the melting and erosion of electrical contacts, either in current interruption with a limited current range of few hundreds of amperes or in making operation under fault condition. For gas-insulated MV-LBS as one of the critical devices in distribution networks, prediction of switch performance at different operational conditions could prolong its lifetime and reliability. The pre-strike arcing time and energy dissipation between the contacts while closing under short-circuit condition could lead to failure in switch operation caused by significant contacts deterioration or even welding [1]. Several studies have been done to optimize MV-LBS with an alternative gas to reduce the use of

SF_6 as an extremely strong greenhouse gas in encapsulated switchgears [2, 3]. A compact air-based MV-LBS is a possible solution for SF6 replacement. However, air is inferior to SF_6 due to a lower dielectric strength, which results in higher pre-strike arcing time and energy dissipation.

Several tens of kiloamperes of short-circuit currents pass through the contacts during making operation in LBS switchgear [1, 4]. The flow of fault current through the switch causes significant contact erosion by raising the temperature, leading to the melting of the contact surfaces, in the worst case, even welding the contacts and failure to re-open [5, 6]. The contacts' surface erosion and melting partly result from absorbing arc energy dissipated while closing the switch [6-8]. Therefore, it is crucial to measure the dissipated arc energy between the contacts while closing under different fault conditions to understand the phenomenon and to avoid switch failure. To reach dissipated arc energy, precise measurement of arc voltage, current, and time are required. The most challenging part of this measurement is direct measurement of arc voltage because of the inherent system response.

In this study, the synthetic circuit is designed to investigate making operation in MV-LBS, which applies a voltage in the order of thousands of volts to make a dielectric breakdown followed by a sharp drop to arc voltage in the order of a few tens of volts. The inherent response of the measurement system, which is normally calibrated using step voltages of hundreds of volts, to this very large step voltage overrides the actual arc voltage. Therefore, an alternative method is required for arc voltage measurement.

As an in-direct measurement method, analysis of arc emission spectroscopy could determine the arc voltage and the dissipated arc energy between the contacts by considering transport properties of arc as air thermal plasma. Besides, Optical Emission Spectroscopy (OES) could provide detailed information on the arc composition by the emitted spectra of excited particles injected into the arc column [9-11]. Metal vapors in the arc could significantly change the arc properties like temperature and conductivity. The information gained from the arc emission spectroscopy is applicable for understanding the metal-arc interface concerning the contact erosion. It provides experimentally measured thermal and electrical properties of the pre-strike arc.

This work characterizes pre-strike arcs by using emission spectroscopy of the arc-contact interface. For this purpose, a test object with a spring-type drive mechanism and a synthetic test circuit are employed. An optical emission spectroscopy set-up is designed to record the temporal evolution of metal vapors close to the contact surface while approaching.

2. Experimental set-up

A test object with a spring-type drive mechanism and a synthetic test circuit is employed. An optical emission spectroscopy set-up is designed to record the temporal evolution of metal vapors close to the contact surface while approaching. The test object is a spring-type switch with axisymmetric arcing contacts made of copper-tungsten (20/80). The stationary contact (cathode) is a 6 mm diameter pin, and the dynamic one (anode) is a tulip with an outer diameter of 15 mm that closes at a speed of 3 m/s. The closing speed and the material type are chosen not to differ significantly from the commercial product. A sensor records the displacement of the dynamic contact over time, making it possible to measure arc length while closing the switch.

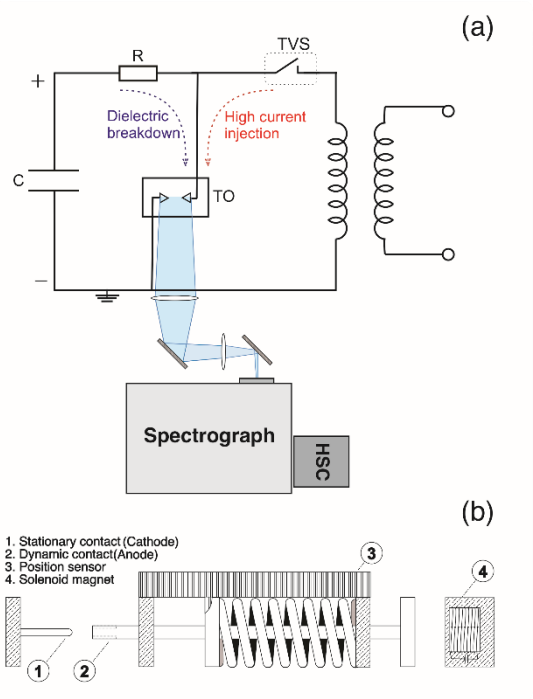

Figure 1. Schematic of the test circuit and spectroscopic set-up (a), and the test-object (b)

Video spectroscopy records the arc composition changes close to the stationary contact surface (cathode). The particle emissions over time are analyzed to investigate pre-strike arc properties. The spectroscopic set-up consists of a spectrograph (Princeton Instrument Acton SP-300i) and a high-speed camera (Photron FASTCAM mini UX50) with 1280×1024 pixels matrix. Figure 1 shows the schematic of the spring type test-object, spectroscopic set-up, and test circuit. The spectrograph has a focal length of 300 mm, 600 lines/mm grating, and slit width of 10 µm. The cathode's front-face is

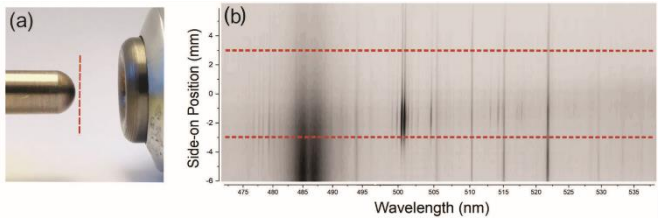

Figure 2. (a) the observation position for arc emission spectroscopy, (b) an example of 2-D spectrum with exposure time of 30 µs recorded during the pre-strike arc.

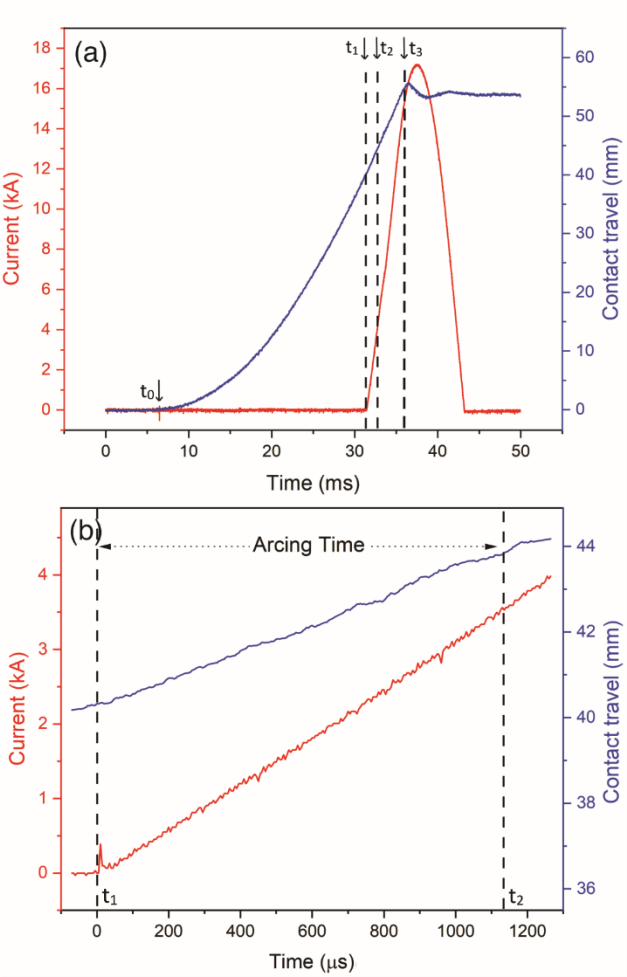

Figure 3. Current waveform and contact travel curve during full making operation (a), and pre-strike arc (b).

imaged to the spectrograph entrance slit (see Figure 2 (a)-dashed line). The recording speed is chosen 25000 fps with an exposure time of 30 µs to reach a proper side-on view and time evolution of the arc while the contacts are approaching. Because of the limited bandwidth in video spectroscopy and the high transition probability of copper species compared to tungsten, the emission spectrum bandwidth of 472-537 nm was chosen to include the major atomic and ionic copper emission lines as required for arc temperature calculation. The spectral and spatial resolutions are ~0.15 nm and ~8 pixels/mm, respectively. Figure 2 (b) shows an example of a two-dimensional image of spectral emission lines.

The test circuit is a synthetic making circuit based on the IEC 62271 standard [12]. The circuit is a combination of synchronized high current and high voltage sub-circuits. The high voltage part makes the dielectric breakdown while contacts are closing. A high-frequency breakdown current is used to trigger the high current circuit to inject the short-circuit current to the test object. A Pearson current sensor measures the arc current. For this study, the test voltage is 18 kV, and the making current is a half-cycle of a 50 Hz sinusoidal current

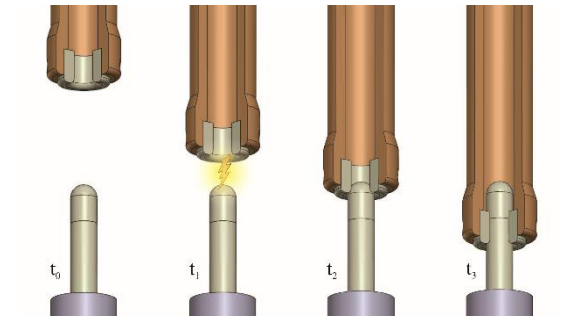

Figure 4. Different stages during making operation-timing is based on the dynamic contact's travel cure

with an amplitude of 17 kA. Figure 3 (a) shows the current waveform and travel curve of the dynamic contacts. The dashed lines show the start and endpoint of the pre-strike arc (t_1-t_2). The arc ignites when contacts are approaching at a distance of ~4 mm and burns for less than 1.2 ms. The fault current in its starting phase, i.e. when the current is between zero and 3.5 kA , flows through the pre-strike arc (t_1-t_2), while the rest of the half-cycle short-circuit current passes through the contacts in closed position where the contacts move through each other between t_2 and t_3, and stop at t_3. Figure 4 shows different stage of contacts position during making operation. The timing corresponds to the travel curve of the dynamic contact shown in Figure 3 (a). Figure 3(b) shows a closer view of the pre-strike arcing time, current, and length. The arc current increases from zero to 3.5 kA during the pre-strike arc. The rest of the short-circuit current flows through zxsthe contacts when they are in touch.

3. Results

In this section, the pre-strike arc temperature is measured by the use of OES. Arc dimension is modeled, which follows by calculation of arc voltage and energy.

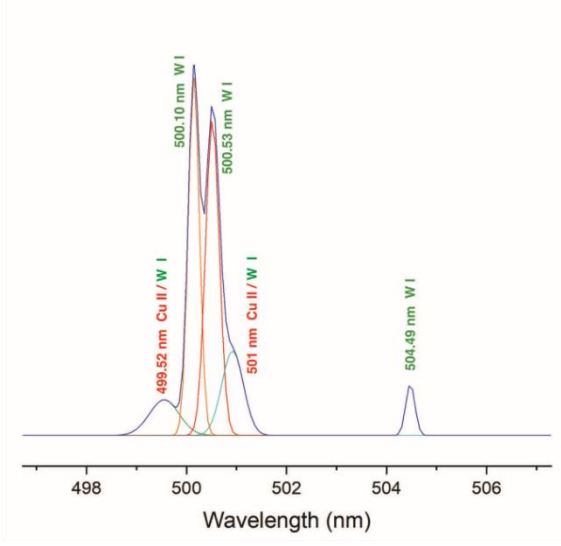

Figure 5. Spectral profile of the first 40 µs of arc burning.

3.1 Optical emission spectroscopy

For emission spectroscopy of the pre-strike arc, the spectrograph slit is aligned perpendicular to the cathode surface (stationary contact) where most injection of metalic particles to the arc column is expected. In Figure 2 (a), the observation window is shown by a red dashed line with a width of twice the pin diameter. A series of two-dimensional spectra is recorded with an exposure time of 30 µs. An example of a recorded 2D image of spectral emission lines is shown in Figure 2 (b). The area limited between red dashed lines shows the pin width (cathode-stationary contact). To get an approach to the arc composition, the spectral lines are determined based on their emission wavelengths. Due to the limited bandwidth of video spectroscopy and high transition probability of copper species compared to tungsten, the emission spectrum center is adjusted to 505 nm with a bandwidth of 65 nm. The chosen wavelength range includes the major atomic and ionic copper emission lines that are required for arc temperature calculation.

The first recorded frame is different from the rest similar to the previous study on the impact of dielectric breakdown low current making operation [13]. The first 40 µs of the arcing time show strong tungsten emission lines at 500.1 and 500.53 nm, indicating air breakdown to initiate the pre-strike arc (see Figure 5). In contrast to the low current making test, an increase in the intensity of the atomic tungsten emissions is observed in the recorded sequence of the pre-strike arc emission spectra in making the short-circuit current. The spectral profile of the pre-strike arc at 240 µs is shown in Figure 6. Besides intense tungsten emission lines at 500.1 and 500.53 nm, more atomic tungsten spectral lines and several atomic and ionic copper spectral lines are recorded, which present the arc composition in the limited chosen bandwidth.

3.2 Boltzmann Plot method

Arc emission spectroscopy determines excitation temperature that can be calculated using Boltzmann plot method if Local Thermal Equilibrium (LTE) condition is given. The method is widely used for plasma temperature measurement [10, 14]. The dependency of integrated intensity I_{ul} of the recorded spectral lines which transmit from upper energy level E_u to lower energy level E_l to plasma temperature T is given by:

$$I_{ul} = \frac{hc}{4\pi\,\lambda_{ul}} A_{ul}\, g_u \frac{n_u}{P} L\, exp\left(\frac{-E_u}{k_B T}\right) \qquad (1)$$

where h is the Planck constant, c is the speed of light, L is the length of the arc, A_{ul} is the transition probability, λ_{ul} is the transition line wavelength, n_u is the number density, P is a partial function, and k_B is the Boltzmann constant. By considering at least two emission lines which are spectrally integrated, the arc temperature can be calculated from inverse slope of Boltzmann Plot. The equation is reduced to:

$$\frac{1}{T} = \frac{k_B}{(E_{u2} - E_{u1})}\, ln\left(\frac{I_1\lambda_1}{g_{u,1}A_{ul,1}} \times \frac{g_{u,2}A_{ul,2}}{I_2\lambda_2}\right) \qquad (2)$$

The chosen spectral lines for equation (2) should have enough excitation energy gap to be used for temperature measurement. Since the equation is derived for a ratio of spectral lines emission intensities, an absolute calibration of the intensities is not required. The applicability of the equation

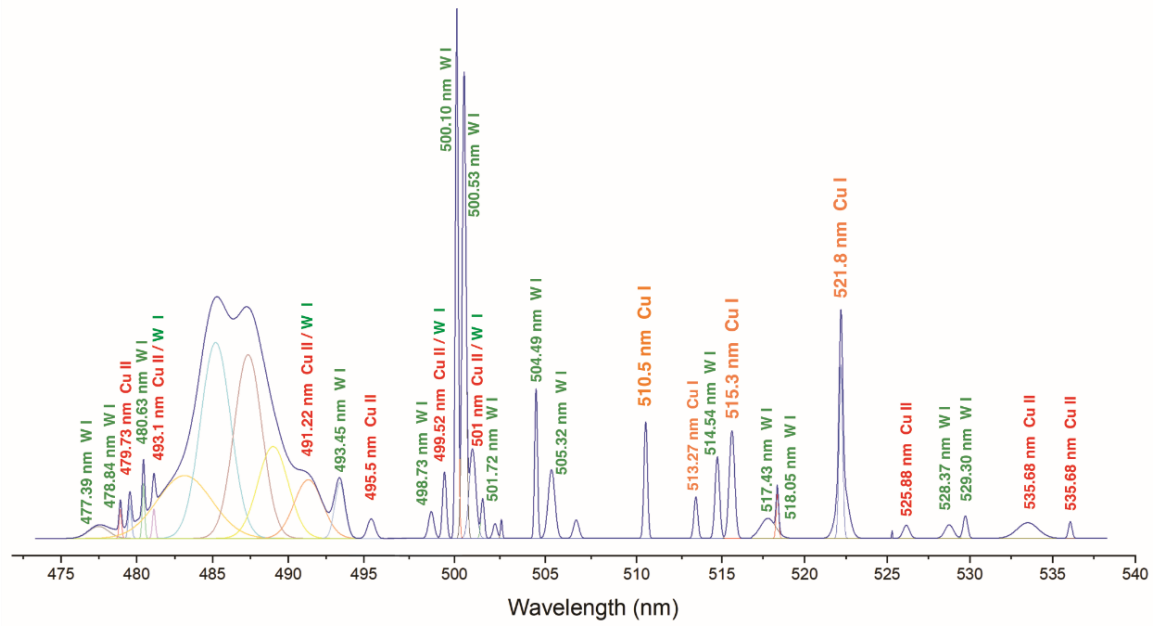

Figure 6. Spectral profile of arc emission at 240 μs with spectral lines corresponds to atomic and ionic copper and atomic tungsten

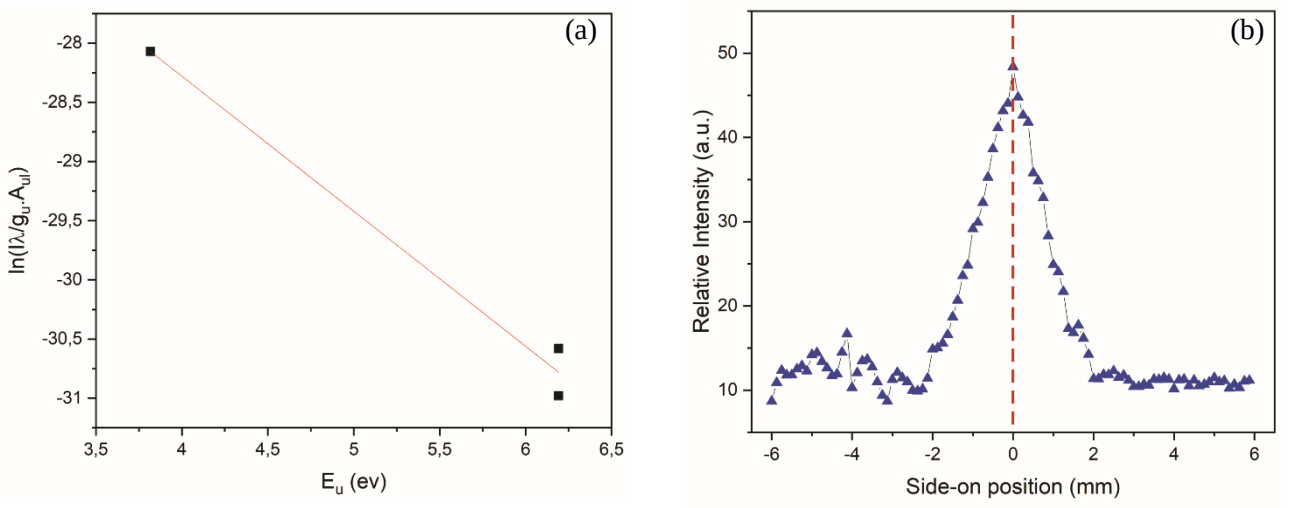

Figure 7. (a) Boltzmann Plot deduced from CuI lines (510.55, 515.32, and 521.82 nm) at 600 μs in the middle of side-on position shows arc temperature of 10168 K, (b) Spectrally integrated relative intensity of CuI emission at 521.82 nm.

is also limited to LTE and optically thin plasma conditions. From visual inspection of the spectra, copper atomic emission lines at 510.55, 515.32, and 521.82 nm are not affected by self-absorption in the most recorded frames. Besides, the energy gap of 2.4 eV between excitation energy levels makes the CuI spectral lines well suited for Boltzmann Plot method-based arc temperature measurement. The spectroscopic parameters for the copper atomic lines are shown in Table 1 taken from NIST atomic database [15]. The arc temperature is obtained by three CuI emission lines using equation (2) at each 40 µs from arc ignition to the contacts touch. Figure 7 (a) shows an example of the Boltzmann Plot from spectrally integrated CuI lines at 600 µs. The plot is made for the middle of side-on position, which is shown in Figure 7 (b) by dashed line. The figure shows the spectrally integrated relative emission of CuI at 521.82 nm. The arc temperature at this point is 10168 K which is calculated as the reverse slope of the line in Figure 7 (a) divided by the Boltzmann constant. The temperature calculation is started at 200 µs because of unacceptable data dispersion for the plot based on the spectrally integrated CuI emission lines for the first 200 µs of the arc burning. From 800 µs, some signs of saturation appeared in the middle of the side-on position at 515.32 and 521.82 nm, which expanded with increasing arcing time until contacts touch moment. The temperature calculation is neglected at these specific positions and is colored black in the temperature profile (Figure 8). The maximum calculated arc temperature is 12500 K, while it could be higher in the black regions. The pre-strike arc temperature distribution shows the arc dynamic motion in time and space. As shown in the temperature profile, the arc ignites in the lower half of the cathode (stationary contact) and moves to the center while the contacts are closing. A temperature drop is observed in the time interval of 400-560 µs before the arc is stabilized in the center, considering the highest temperature in the center of the arc column. The contact movement could cause the arc to cool during the closing operation by creating a gas flow blowing the arc. It has to be mentioned that the periodic discontinues pattern observed at 360 µs of the temperature profile is because of electromagnetic noises interfere with the recording system.

For reproducibility, a few tests have been conducted under the same test conditions. Similar arc composition and approximately equal species emission line intensities have been observed. The difference is in the spatial distribution of

Table 1. Spectroscopic data for atomic copper emission lines used for temperature measurement

Wavelength (nm)	Upper-level E (eV)	Lower-level E (eV)	Upper-level degeneracy	Transition probability (s^{-1})
510.55	3.817	1.389	4	2.0×10^{6}
515.32	6.191	3.786	4	6.0×10^{7}
521.82	6.192	3.817	6	7.5×10^{7}

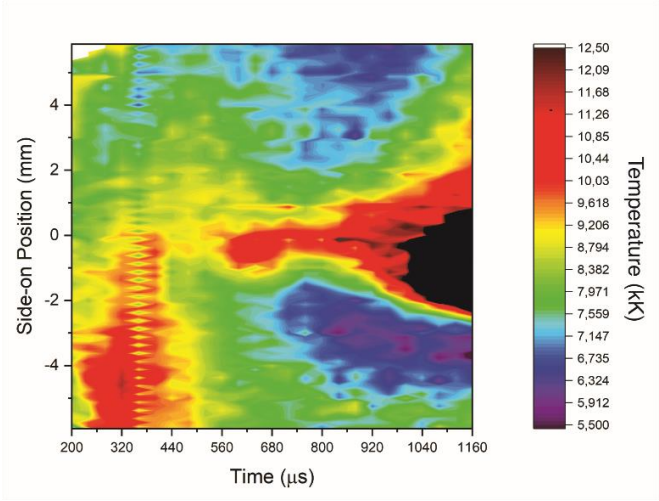

Figure 8. Temperature profile of pre-strike arc for 18 kV breakdown voltage and 17 kA fault current (50 Hz)

emission lines in the side-on position for the first 500 µs because the arc ignites randomly at different spots of the contact surface. The rest of the arc burning time ends up with similar coherent temperature behavior in all the tests like the arc temperature shown in Figure 8 between 500 and 1160 µs.

3.3 Electrical characteristics of pre-strike arc

The dissipated arc energy between the contacts is partly absorbed by the contacts surfaces, which could heat them up to the melting and evaporation points. Therefore, measuring the dissipated energy could provide an appropriate measure of the contacts erosion and welding. The energy could be obtained by arc voltage and current measurement. The arc current is measured experimentally. Challenges exist regarding arc voltage measurement. A distortion in voltage waveform is observed in the direct measurement of the pre-strike arc voltage because of the inherent response of the measurement system to the large step voltage caused by a breakdown in the switch (in this case, a step voltage of 18 kV). An alternative method obtains the pre-strike arc voltage using arc temperature and applying thermal air plasma transport properties in atmospheric pressure. Numerical simulation studies exist on temperature dependency of electrical conductivity for dry air plasma at atmospheric pressure [16-18]. The electrical conductivity is obtained by tracing electrical conductivity as a function of temperature at LTE condition (Figure 9). By assuming the pre-strike arc as dry thermal air plasma, electrical conductivity is calculated as shown in Figure 10. The maximum calculated conductivity is 5300 S/m. The conductivity is not determined for black regions due to the lack of data for arc temperature. Since the electrical conductivity in dry air thermal plasma at atmospheric pressure increases approximately linearly with temperature (for temperatures less than 25000 K) and the arc temperature is expected to be higher than 12500 K in black regions, the electrical conductivity should be higher than 5300 S/m in these areas.

There is no clear information on the percentage of metal vapor in the arc column because of the spectrograph's limited bandwidth. Therefore, the electrical conductivity is also carried out for 100% saturated thermal air plasma with copper in addition to pure thermal air plasma, which makes it possible to discuss the pre-strike arc electrical characteristics in a range of copper perecentage impurity.

To calculate the electrical characteristics of pre-strike arc, it is necessary to estimate the arc dimension. Assuming that the pre-strike arc is cylindrically shaped, the arc length can be approximately determined by using the travel curve of the dynamic contact (see Figure 3). For the cross-sectional area, Lowke's analytical model of free-burning arcs is employed [19]. The model is based on theoretical prediction and experimental measurements of high current arcs at atmospheric air pressure. The arc radius expression is derived

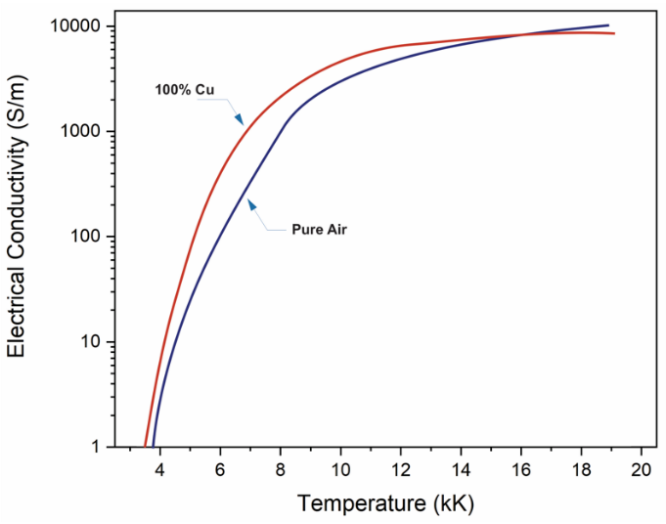

Figure 9. Electrical conductivity as a function of temperature for dry thermal air plasma and 100% saturated with copper vapor adapted from [16].

from the conversion equations for energy (3) and momentum (4):

$$I^2/\sigma A^2 = 4\pi kT/A + U \quad (3)$$

$$\rho v dv/dz = -\rho g - (dp/dz) \quad (4)$$

wherein equation (1) I is the arc current, σ is the electrical conductivity, k the thermal conductivity, and U the net radiation emission coefficient. In equation (2), ρ is the density of the plasma, p the pressure, υ the plasma axial velocity, z axial position, and g the gravity. However, in high current arc density, the radiation loss term (U) is dominant over the conduction term (4πkT/A) because of the high magnetic conduction. The term dp/dz arises due to the magnetic constriction effect on P. Therefore, the term ρg is omitted, which is smaller than dp/dz.

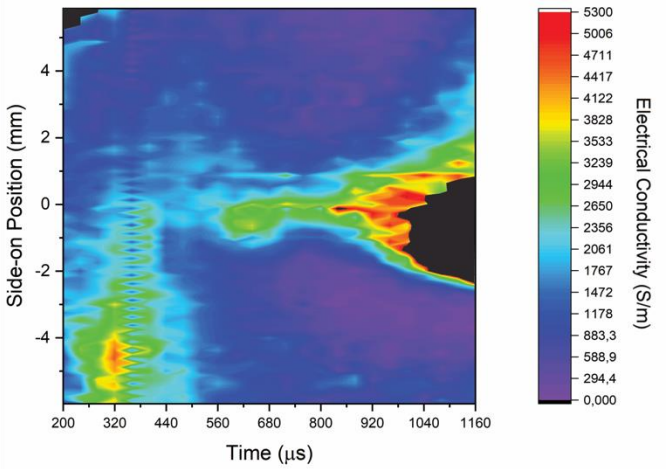

Figure 10. Pre-strike arc electrical conductivity as dry air thermal plasma

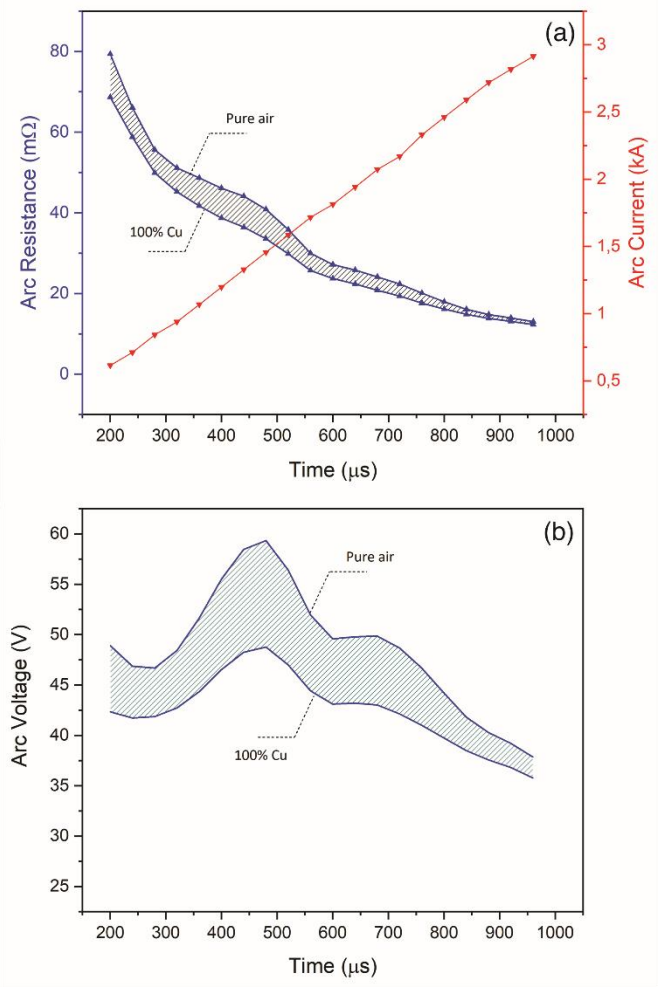

Figure 11. Electrical characteristics of the pre-strike arc influenced by metal vapors when the arc is free of vapor and 100% saturated with copper vapor. (a) arc resistance and current, (b) arc voltage

Considering more approximations regarding radial pressure, radiation, viscous and turbulence losses, the arc radius is obtained by Lowke as:

$$R = 1.11 \left(\frac{Z}{h\sigma}\right)^{\frac{1}{4}} I^{\frac{3}{8}} \Big/ (\mu j_0 \rho)^{\frac{1}{8}} \qquad (5)$$

where h is enthalpy and μ=0.126 dyne/A^2. The agreement of the theory and experiment by Lowke is an evidence that j_0 is constant with current, otherwise the theoretical predictions differ markedly from experiments. Therefore, an estimated error of 20% is considered because of uncertainty in the value of j_0.

Considering the experimentally measured electrical conductivity, the values of enthalpy and density are taken from Capitelli et al. database on thermal air plasma transport properties at atmospheric pressure in the temperature range 50-30000 K [18]. For the sake of accuracy, the electrical characterization is carried out for the arcing time of 200 to 920 μs when OES measures a decent pre-strike arc temperature, and the calculation is neglected for the regions whereby saturation in the CuI emission lines is observed (black regions). In this case, the arc radius is changing in the range of 2.3-3.3 mm.

The arc resistance is calculated by the electrical conductivity concluded from arc temperature and the arc dimension with respect to the anode travel curve and the Lowke model. The arc voltage is obtained using arc resistance and experimentally measured arc current. We should notice the calculated arc voltage does not include a voltage drop across the plasma sheath in front of the contacts. The minimum arc voltage for tungsten and copper as the electrical contact material is measured 13.5 and 13 V, respectively [20]. Since the majority of the contacts material is tungsten (80% tungsten, 20% copper), the minimum arc voltage is considered 13.5 V. The arc resistance and voltage including cathodic voltage drop as a function of time are shown in Figure 11 (a) and (b), respectively. By considering the impact of copper vapor density in arc conductivity [18], the resistance, and the voltage could be limited to the area bounded by two curves shown Figure 11 where the arc is free of copper vapor or 100% saturated with copper vapor.

A comparison between the calculated pre-strike arc voltage and free-burning arc voltage at different distances shows that reasonable voltage values are obtained.

Although we expect the arc voltage to decrease with increasing arc burning time, based on the earlier studies [21, 22], there is an increase in arc voltage while the arc current is linearly increasing. At the same moment of voltage increasing, the arc resistance curve shows almost constant values in Figure 11, and the temperature profile shows the arc moving from the lower part of the stationary contact to the center where the arc evolution looks stable until contacts touch moment.

4. Discussion

Understanding the pre-strike arc behavior during making operation under a fault condition is crucial for improving load break switches concerning contacts erosion. The same approach is necessary for earthing switches in short-circuit fault levels, which shows this investigation's necessity. The dissipated energy due to arc burning between the contacts while closing could be proportional to the degree of contact erosion and welding. The arc energy can be determined by the arc voltage and current over arcing time. There are some challenges regarding this measurement. In the direct measurement of the pre-strike arc voltage, a distortion in voltage waveform is observed due to the measurement system's inherent response to the large step caused by a breakdown in the switch (in this case, a step voltage of 18 kV). Therefore, the pre-strike arc voltage is calculated indirectly using arc temperature measured by OES and the arc

parameters database for atmospheric pressure air thermal plasma. There are some limitations regarding the observation window position in arc spectroscopy when there is a moving contact, which makes it difficult to scan the whole arcing time evolution because it partly burns inside the dynamic tulip contact before touch moment. Therefore, the arc voltage is approximately estimated at these moments based on the adjacent electric field and the arc length. A comparison of the indirectly calculated pre-strike arc voltage with free-burning arc voltage at different distances shows that the obtained voltage values are reasonable. The dissipated energy between the contacts during 1.2 ms pre-strike arc burning could range from 79 to 87 joules.

From the temperature profile of the pre-strike arc, information on arc dynamic motion is concluded. It can be seen that the arc evolution is different from the free-burning arc [21, 22]. The arc is unstable for the first 500 μs of burning. Afterward, it gradually gets stable and expands in the center of the arc column. A temperature fall happens before the arc starts expanding in the center, caused by arc cooling because of gas flow through the contact movement. The enhanced cooling at this time can be observed as an increase in the arc voltage. Reducing the arcing time by closing the contacts faster could be an idea to reduce the impact of prestrike arc on contacts erosion.

Another factor that has a direct impact on dissipated energy between contact is insulation gas. This study is done in air as an alternative to SF_6. Some additives could be mixed with air to increase its dielectric strength and reduce the arcing time under making operation to reduce the pre-strike arc dissipated energy. The proposed investigation method in this study could also be used to detect arc decomposition by-products concerning the environmental compatibility of different gas mixtures, as well as for the investigation of switching arc properties under different fault conditions.

5. Conclusion

In summary, pre-strike arc characteristics during the making of short-circuit current in an air MV-LBS model switch is investigated by arc emission spectroscopy. The arc dynamic motion concluded from the temperature profile shows the contact movement cooling impact in arc behavior. Because of the distortion in the direct measurement of arc voltage, the arc voltage and subsequently, the dissipated energy between contacts during making operation are measured using OES. We consider the influence of metallic vapor in the arc voltage. From the pre-strike arc characterization. The proposed method could be a proper diagnostic to understand the physical mechanisms involved in the making operation of MV-LBS, and the performance of the switching device.

Acknowledgment

The work was financially supported by the Norwegian Research Council, grant # 269361. The authors would like to thank Bård Ålmos and Morten Flå from NTNU for technical supports.

References

[1] Niayesh K and Runde M 2017 *Power Switching Components* (Cham, Switzerland: Springer)
[2] Støa-Aanensen N S, Runde M, Jonsson E and Teigset A 2016 *IEEE Transactions on Power Delivery* **31** 278-85
[3] Taxt H, Niayesh K and Runde M 2019 *IEEE Transactions on Power Delivery* **34** 2204-10
[4] Seeger M 2015 *Plasma Chemistry and Plasma Processing* **35** 527-41
[5] Pons F and Cherkaoui M 2008 An electrical arc erosion model valid for high current: Vaporization and Splash Erosion. In: *2008 Proceedings of the 54th IEEE Holm Conference on Electrical Contacts*: IEEE) pp 9-14
[6] Mohammadhosein M, Niayesh K, Shayegani-Akmal A A and Mohseni H 2018 *IEEE Transactions on Power Delivery* **34** 580-7
[7] Kadivar A and Niayesh K 2019 *Journal of Physics D: Applied Physics* **52** 404003
[8] Zhang J L, Yan J D and Fang M T 2004 *IEEE Transactions on Plasma Science* **32** 1352-61
[9] Hartinger K, Pierre L and Cahen C 1998 *Journal of Physics D: Applied Physics* **31** 2566
[10] Valensi F, Pellerin S, Boutaghane A, Dzierzega K, Zielinska S, Pellerin N and Briand F 2010 *Journal of Physics D: Applied Physics* **43** 434002
[11] Khakpour A, Methling R, Franke S, Gortschakow S and Uhrlandt D 2018 *Journal of Applied Physics* **124** 243301
[12] IEC S 2006 62271-101. In: *High-Voltage Switchgear and Controlgear–Part 101: Synthetic Testing*,
[13] Dorraki N and Niayesh K 2020 *IEEE Transactions on Plasma Science* **48** 3698-704
[14] Unnikrishnan V, Alti K, Kartha V, Santhosh C, Gupta G and Suri B 2010 *Pramana* **74** 983-93
[15] NIST Atomic Spectra Database Lines Form. Accessed: Dec. 21, 2020. [Online]. Available: https://physics.nist.gov/PhysRefData/ASD/lines_form.html.
[16] Cressault Y, Hannachi R, Teulet P, Gleizes A, Gonnet J and Battandier J 2008 *Plasma Sources Science and Technology* **17** 035016
[17] Murphy A B and Arundelli C 1994 *Plasma Chemistry and Plasma Processing* **14** 451-90
[18] Capitelli M, Colonna G, Gorse C and d'Angola A 2000 *The European Physical Journal D-Atomic, Molecular, Optical and Plasma Physics* **11** 279-89
[19] Lowke J 1979 *Journal of physics D: Applied physics* **12** 1873
[20] Slade P G 2017 *Electrical contacts: principles and applications* (Boca Raton, FL, USA: CRC press)
[21] Lowke J, Kovitya P and Schmidt H 1992 *Journal of Physics D: Applied Physics* **25** 1600
[22] Baeva M, Uhrlandt D, Benilov M and Cunha M 2013 *Plasma Sources Science and Technology* **22** 065017